

# Miniaturized High-Pass Filter Based on Balanced Composite Right-Left Handed Transmission Line Using Meander Spiral Complementary Split Ring Resonators

Esmail Zarezadeh<sup>1</sup>, Hossein Fathabadi<sup>1</sup> and, Mostafa Danaeian<sup>2</sup>

<sup>1</sup>Department of Electrical Engineering, Khatam-al-Anbia University, Tehran, Iran.

<sup>2</sup>Department of Electrical Engineering, Vali-E-Asr University of Rafsanjan, Kerman, Iran.

zarezadeh@aut.ac.ir, h.fathabadi@gmail.com, m.danaeian@gmail.com

Corresponding author: m.danaeian@gmail.com

**Abstract-** In this paper, a compact high-pass filter (HPF) with a sharp rejection response based on the balanced composite right-left handed (CRLH) transmission line (TL) concept is proposed. A series LC resonator using an interdigital capacitor and meander lines is designed. Also, a meander spiral complementary split ring resonator (MSCSRR) is used to realize the parallel LC resonator. The high-pass filter is implemented in microstrip technology by etching MSCSRR, in the ground plane, and series interdigital capacitor with meander lines, in the signal strip. Because of a smaller electrical size of the proposed MSCSRR and also by using meander lines instead of conventional transmission lines, the total physical dimension of the proposed high-pass filter has been reduced. A detailed analysis of the structure, based on the equivalent circuit model is provided. The structure exhibits a balanced CRLH behavior and by properly tuning the geometry of the elements, a high-pass response with a sharp transition band is obtained. To validate the design concept, the proposed high-pass filter has been fabricated and tested. Experimental verification is provided and a good agreement has been found between the simulation and measurement results. To our knowledge, the size of proposed HPF is more compact in comparison with known similar filters.

**Index Terms-** metamaterial, balanced composite right-left handed transmission line (CRLH TL), meander, meander spiral complementary split ring resonator (MSCSRR), high-pass filter (HPF), and compact size.

## I. INTRODUCTION

The double negative (DNG) structures, especially composite right/left handed (CRLH) structures, make a great interest in the microwave engineering based on their unusual properties [1-3]. DNGs are artificial materials with negative permittivity and permeability, simultaneously. DNG structures are

widely used to improve the performance of microwave circuits. Although the electromagnetic properties of the left handed metamaterial has been predicted by Veselago [1-3] in the late sixties however, such a media were not artificially fabricated until 2000 [2]. Artificial metamaterial transmission lines have been applied to the design of microwave devices, such as power divider, couplers, phase shifters, and filters [1–3]. The CRLH TL are constituted of series capacitors  $C_L$  and shunt inductors  $L_L$ , intended to provide left-handed TLs, whereas the contributions  $C_R$  and  $L_R$  come from their parasitic reactances and have an increasing effect with increasing frequency. The parasitic inductance  $L_R$  is due to the magnetic flux generated by the currents flowing along the digits of the capacitor and the parasitic capacitance  $C_R$  is due to the parallel-plate voltage gradients existing between the top layer and the ground plane.

Broadly speaking, two main approaches exist to obtain the left-handed transmission lines. One of them is the dual transmission line approach [1-3], which is based on loading transmission lines with series capacitances and shunt inductances. The other one is the resonant-type approach [1-3], which combines resonant sub-wavelength particles, such as split rings resonators (SRRs) or their dual counterparts (CSRRs), with shunt inductances or series capacitances etched on a host transmission line.

Filtering unwanted signals is an essential function of many electronic systems, including commercial and military platforms such as communications, electronic-warfare (EW), and radar systems. One of the choices for the filter responses is the high-pass filter, which suppresses signals in lower frequencies and ideally passes signals in higher frequencies. High-Pass filters based on the metamaterial transmission lines have been investigated in microstrip, coplanar waveguide (CPW), and monolithic microwave integrated circuit technologies [5–9].

In this paper, a high-pass filter based on the balanced metamaterial TL concept, using an interdigital capacitor with meander lines as a series resonant tank and a meander spiral CSRR (MSCSRR) as a parallel resonant tank is designed. In the proposed design, the series capacitor  $C_L$  is realized by interdigital capacitor. This capacitor is a multi-finger periodic structure which uses the capacitance that occurs across a narrow gap between thin-film conductors. The series inductors  $L_R$  for RF applications, realized by meander lines. The shunt inductor  $L_L$  and shunt capacitor  $C_R$  are provided by the MSCSRR which is etched in ground plane. To verify the proposed method, the designed high-pass filter has been fabricated and measured. Simulation and measurement results are carried out to prove the validity of the proposed filter. Good agreement between their simulated and measured results have been achieved. In comparison with the previous works, because of the small physical size of the MSCSRR, our proposed microstrip filter is very compact.

## II. DESIGN PROCEDURE

The canonical circuit models of the metamaterial unit-cell are shown in Fig. 1. These circuit models

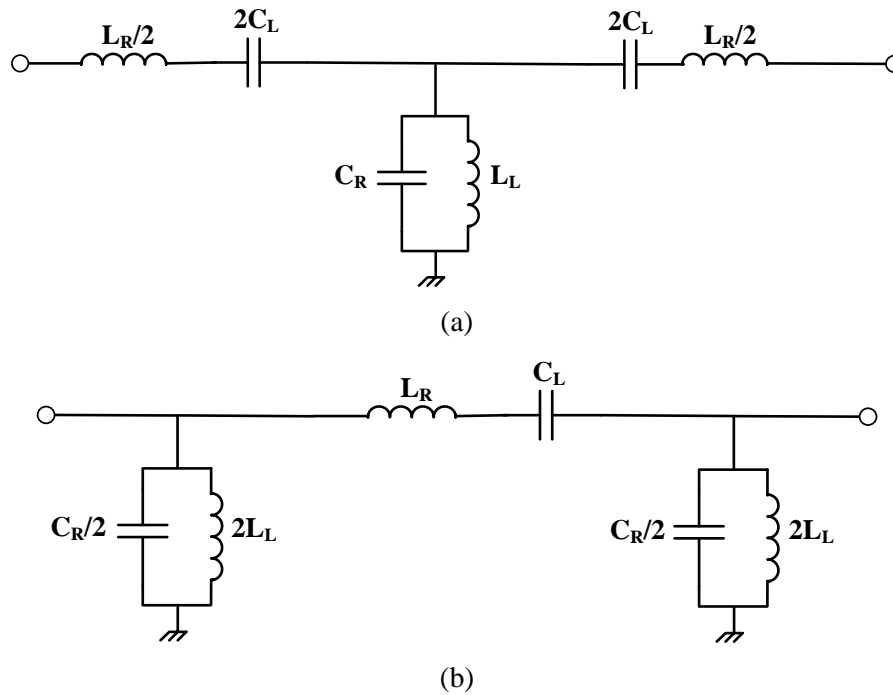


Fig. 1. Canonical circuit model of a metamaterial transmission line unit-cell, (a) T-model, (b)  $\pi$ -model.

are the T- and  $\pi$ -circuits, where the shunt branch is a parallel resonant tank, and the series branch is a series LC resonator. A balanced metamaterial unit-cell has identical series and shunt resonances namely:

$$\omega_{se} = \omega_{sh} \Rightarrow L_R C_L = L_L C_R \Rightarrow Z_L = Z_R \tag{1}$$

To realize a high-pass filter based on the balanced metamaterial unit-cell concept, a parallel LC resonator is needed. MSCSRR are very suitable components to realize pure parallel resonators. A MSCSRR is designed at the central frequency ( $f_0$ ). For realizing the series resonant tank, an interdigital capacitance as a capacitor and two meander lines as inductors are used. Fig. 2 shows the layout of the series resonant tank and its simple circuit model. In this model, the interdigital capacitor is modeled with a capacitor and two parasitic capacitances, and the meander line is modeled with an inductance. An interdigital capacitor that has a value equal to  $2C_L$  should be designed. An interdigital capacitor cannot obtain a pure capacitance and has two parasitic capacitances ( $C_p$ ) as shown in Fig. 2, which can be neglected. After extracting the parasitic capacitances of the designed interdigital capacitance, the value of inductance in the series resonator should be calculated. To this end, the series resonant tank is forced to exhibit the resonance at  $f_0$ . The analysis of the structure can be driven through Bloch theory. The phase shift per cell,  $\varphi = \beta l$ , and the characteristic impedance,  $Z_B$ , which are the key parameters for microwave circuit design, are given by [4].

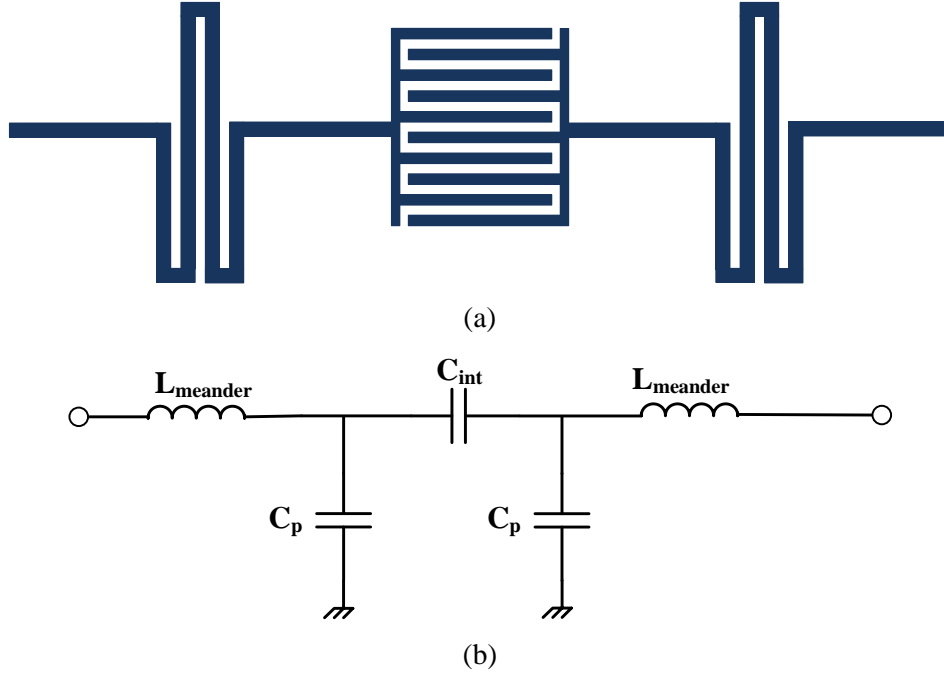


Fig. 2. Layout of the series resonant tank consisting of an interdigital capacitance and two meanders and a simple circuit model.

$$\cos \varphi = \cos \beta l = 1 + \frac{Z_S(\omega)}{Z_P(\omega)} \quad (2)$$

$$Z_B = \sqrt{\frac{Z_S(\omega)Z_P(\omega)/2}{1 + Z_S(\omega)/2Z_P(\omega)}} = \sqrt{\frac{Z_S(\omega)Z_P^2(\omega)}{2Z_P(\omega) + Z_S(\omega)}} \quad (3)$$

where  $Z_S$  and  $Z_P$  are the series and shunt impedances, respectively. Propagation is allowed in that region where both  $Z_B$  and  $\varphi$  are real numbers.

Let us now analyze in detail the dispersion diagram and the dependence on frequency of the characteristic impedance. Two different conditions will be considered: 1) the unbalanced case, and 2) the balanced case. Accordingly, the metamaterial unit-cells can be designed to be either unbalanced or balanced [4]. In the first case, the series impedance and shunt admittance are null at different frequencies. Conversely, the series and shunt resonance frequencies are identical for balanced designs. Thus, for unbalanced structures, a frequency gap appears between the following frequencies:

$$\begin{aligned} f_{g1} &= \min(f_S, f_P) \\ f_{g2} &= \max(f_S, f_P) \end{aligned} \quad (4)$$

where  $f_S$  and  $f_P$  are the series and shunt resonance frequencies, respectively, and the structure is left/right-handed below/above that gap. For the balanced case, these frequencies are identical, namely,  $f_S = f_P = f_0$ , and the transition between the left and right-handed band is continuous (i.e., it takes place

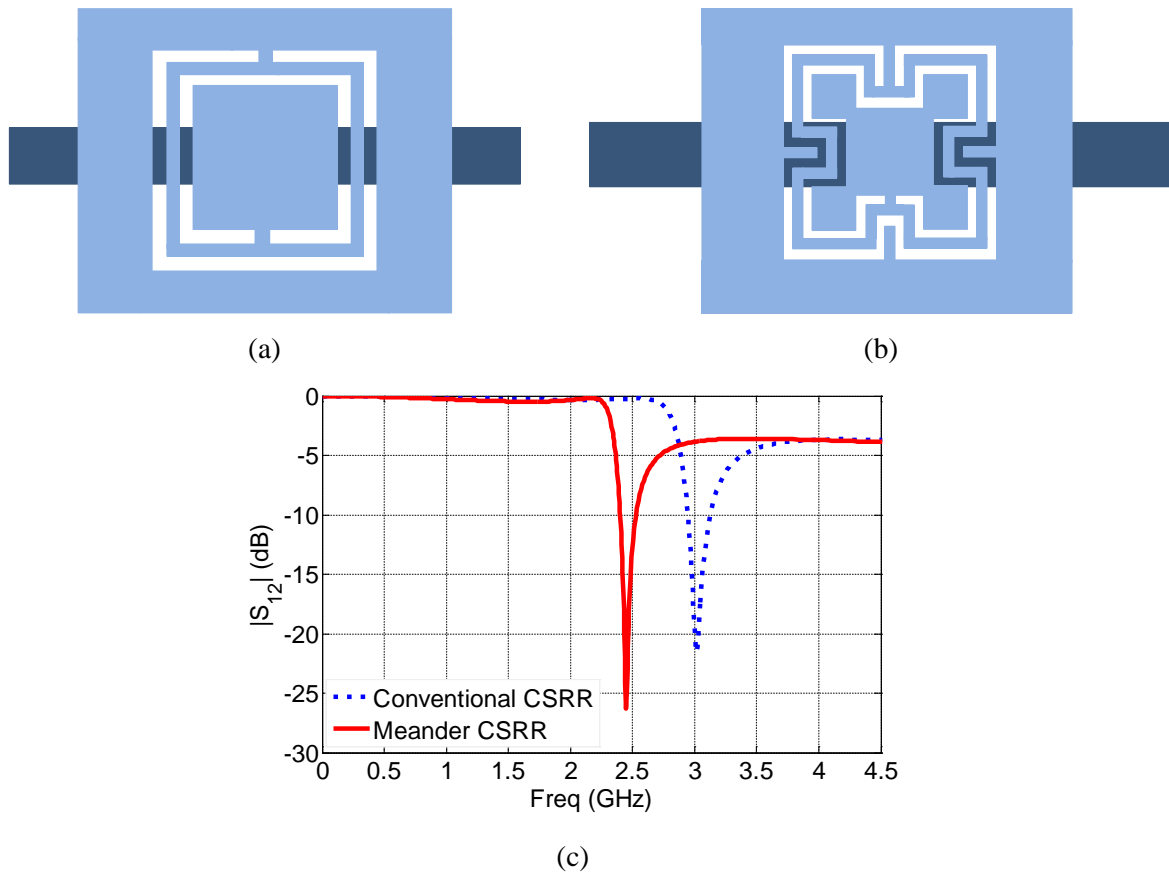


Fig. 3. Test structure for demonstrating the ability of the proposed MSCSRR unit cell to miniaturization of the size, based on a microstrip loaded with (a) The conventional CSRR unit cell, (b) The proposed MSCSRR unit cell and (c) Simulated frequency response of them.

at the transition frequency  $f_0$ ).

In order to demonstrate the achievable broadband characteristics of MSCSRR-loaded CRLH transmission lines, a one-cell balanced structure has been designed and simulated. The transition frequency has been set to  $f_0 = 1.34$  GHz. To determine MSCSRR dimensions, the formulas given in [6] have been used. Gap and line dimensions have been estimated from standard formulas. Optimization has been required since the expressions given in [6] are valid under restrictive conditions, not strictly of application in the structures under study. Thus, MSCSRR dimensions have been scaled until the impedance seen from the ports has been found to be located in the unit resistance circle of the Smith Chart at  $f_0$ .

By etching the proposed MSCSRR unit cell in the ground plane of a microstrip transmission line, due to the negative effective permittivity in the vicinity of the resonance frequency of the MSCSRR, the signal is inhibited in a narrow band [1-3]. Fig. 3 illustrates such structure, where one conventional CSRR and one MSCSRR is etched in the ground plane. The simulated frequency response for these devices is depicted in Fig. 3(c). As can be seen in Fig. 3(c), a stopband appears in the vicinity of  $f_0 = 3$

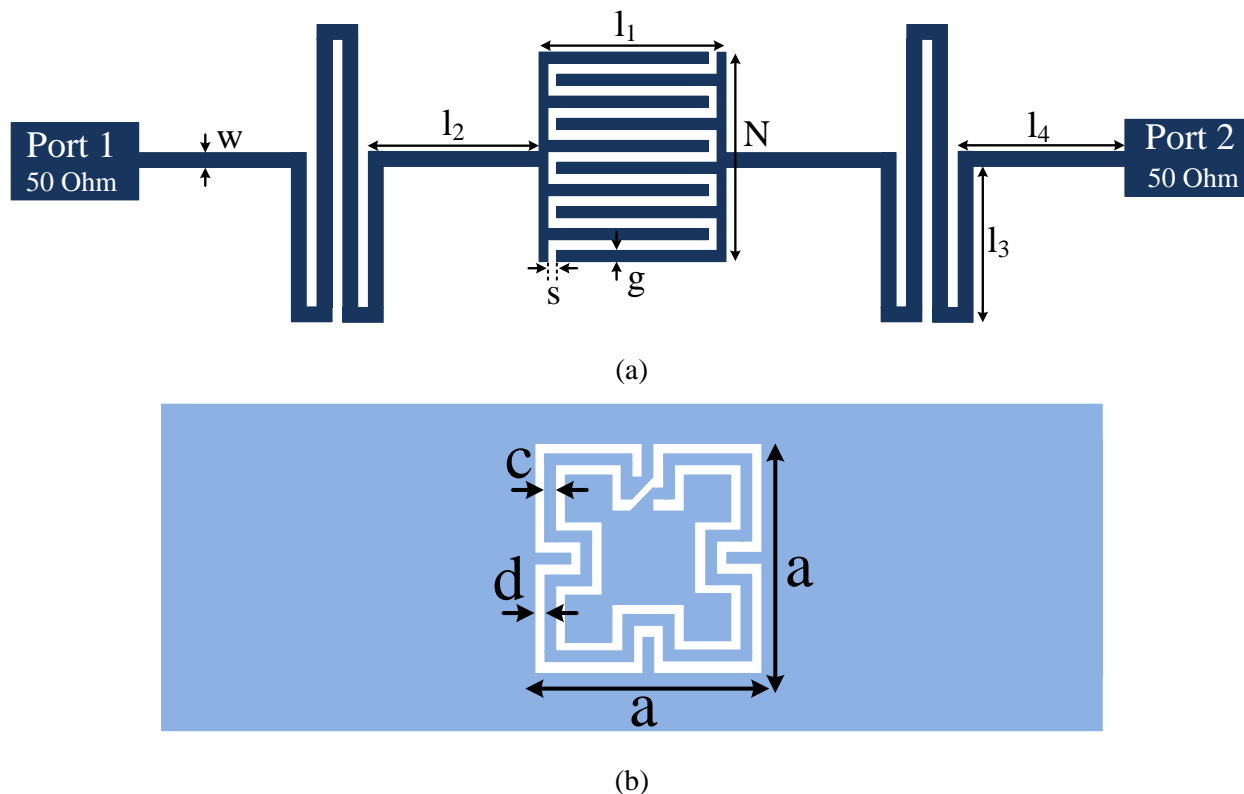


Fig. 4. Configurations of the proposed filter. (a) Top and (b) bottom layers.

GHz for the conventional CSRR structure while this stopband appears in the vicinity of  $f_0 = 2.4$  GHz for the proposed MSCSRR structure. Fig. 3(c) illustrate that the electrical size of the MSCSRR unit cell is larger than the conventional CSRR unit cell with the same size. Therefore, by using the MSCSRR instead of the conventional CSRRs, a miniaturization factor about 0.25 is achieved, which demonstrate the ability of the proposed unit cell to decrease the size.

Configurations of the proposed high-pass filter (Top and bottom layers) is shown in Fig. 4. The synthesis of left-handed transmission lines by properly etching MSCSRR in the back substrate is possible [4]. In contrast to the dual transmission line approach, this approach is called the resonant-type approach, because resonators (MSCSRRs) are utilized as loading elements. It is important to note that the resonant type metamaterial transmission lines also exhibit a composite right-left handed (CRLH) behavior.

The high-pass filter is implemented in microstrip technology by etching meander spiral complementary split ring resonators (MSCSRR), in the ground plane, and series capacitive gaps, or interdigital capacitors, in the signal strip. An interdigital capacitors is a multi-finger periodic structure which can be used as a series capacitor in microstrip transmission lines technology [4]. An interdigital capacitor is made of some gaps. The gap meanders back and forth in a rectangular area forming two sets of fingers that are interdigital. These gaps are essentially very long and folded to use a small

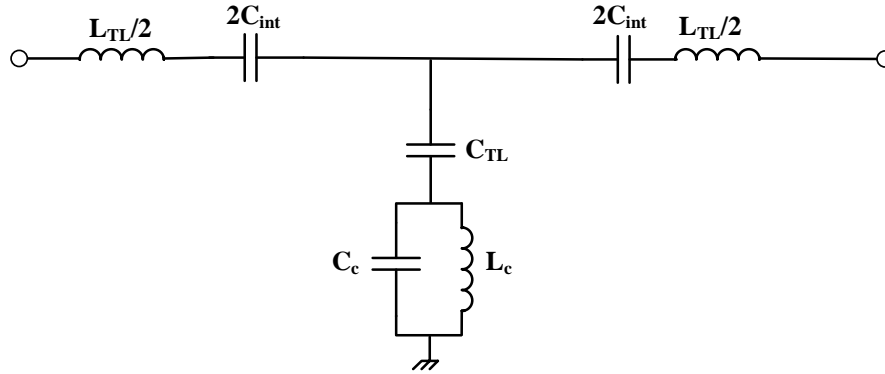


Fig. 5. Equivalent circuit model of the proposed High-Pass filter.

amount of area. By using a long gap in a small area, compact series capacitors can be realized. Consequently, the structure exhibits a composite right/left handed (CRLH) behavior and, by properly tuning the geometry of the elements, a high-pass response with a sharp transition band is achieved. The high selectivity of these microwave filter is due to the presence of a transmission zero. This property is a clear advantage, as it implies a smaller electrical size at resonance. On the other hand, since the resonance frequency of the proposed MSCSRR with two turn is lower than the resonance frequency of the conventional CSRR with the same size, therefore by using the MSCSRR more miniaturization is obtained. Accordingly, due to the small size of the resonant elements, the total dimension of the proposed high-pas filter is very compact.

The proposed high-pass filter structure is described by means of the circuit model shown in Fig. 5, where the MSCSRR is modeled by the resonant tank formed by the capacitance  $C_c$  and the inductance  $L_c$ , whereas the interdigital capacitor is described through the capacitance  $C_{int}$ .  $L_{TL}$  is the inductance of the meander lines, whereas  $C_{TL}$  accounts for the line capacitance and the fringing capacitance of the interdigital capacitor, and it models the electric coupling between the line and the MSCSRRs.

Fig. 6 represents the results obtained from circuit models and full-wave simulations, which verifies our prediction. The resulting element values of the circuit model for the designed HPF are:  $L_{TL}=4.4$  nH,  $C_{TL}=4.30$  pF,  $C_c=1.9$  pF,  $L_c=3.5$  nH,  $C_{int}=1.35$  pF.

According to the equivalent-circuit model, the transmission zero, given by that frequency which nulls the shunt branch, that is:

$$f_z = \frac{1}{2\pi\sqrt{L_c(C_c + C_{TL})}} \tag{5}$$

As well as, the general expression providing the phase shift per cell and the characteristic impedance are given by:

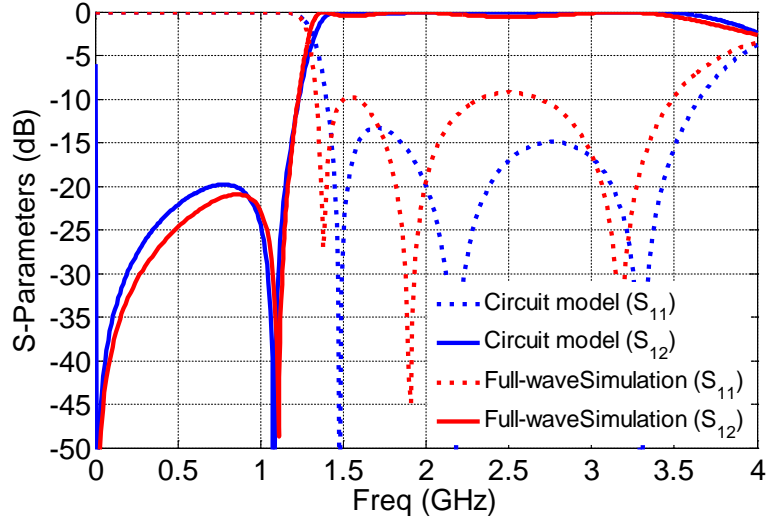


Fig. 6. EM-simulated and circuit model S-parameters of the proposed HPF.

$$\cos \phi = \frac{2\omega(\omega^2 - \omega_p^2) + 2\omega^3 \omega_p^2 L_c C_{TL} + (\omega^2 - \omega_s^2)(\omega_p^2 - \omega^2) L_{TL} C_{TL}}{2(\omega^2 - \omega_p^2) + 2\omega^3 \omega_p^2 L_c C_{TL}} \quad (6)$$

$$Z_B = \sqrt{\frac{L_{TL} \left(1 - \frac{\omega_s^2}{\omega^2}\right)}{C_c \left(1 - \frac{\omega_p^2}{\omega^2}\right)} - \frac{L_{TL} \omega^2 \left(1 - \frac{\omega_s^2}{\omega^2}\right)^2}{4} + \frac{L_{TL} \left(1 - \frac{\omega_s^2}{\omega^2}\right)}{C_{TL}}} \quad (7)$$

Where these expressions for the balanced case are simplified to

$$\cos \phi = \frac{2\omega(\omega^2 - \omega_0^2) + 2\omega^3 \omega_0^2 L_c C_{TL} - (\omega^2 - \omega_0^2)^2 L_{TL} C_{TL}}{2(\omega^2 - \omega_0^2) + 2\omega^3 \omega_0^2 L_c C_{TL}} \quad (8)$$

$$Z_B = \sqrt{\frac{L_{TL}}{C_c} - \frac{L_{TL} \omega^2 \left(1 - \frac{\omega_0^2}{\omega^2}\right)^2}{4} + \frac{L_{TL} \left(1 - \frac{\omega_0^2}{\omega^2}\right)}{C_{TL}}} \quad (9)$$

The normalized dispersion relation and the curve of the attenuation constant for the proposed filter are shown in Fig.7. The dispersion diagram exhibits a negative slope at the frequencies of interest, which confirms the backward-wave nature of the passband. As well as, the curve of the attenuation constant shows that the attenuation constant is zero in the observed frequency range.



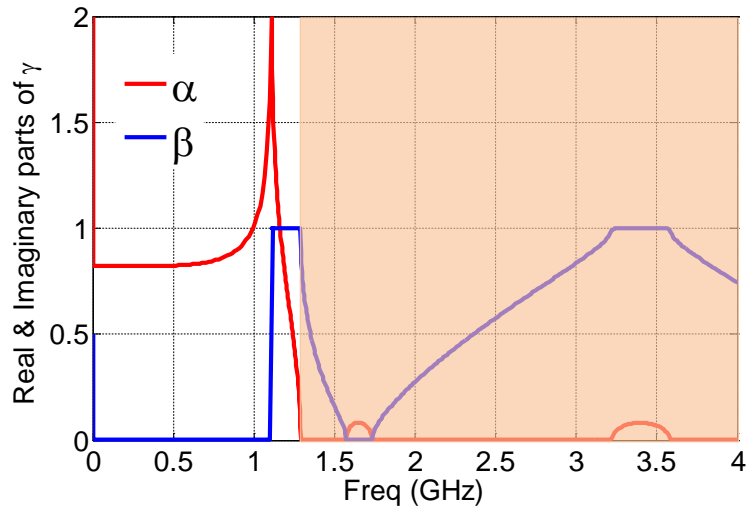


Fig. 7. Dispersion diagram of the proposed filter.

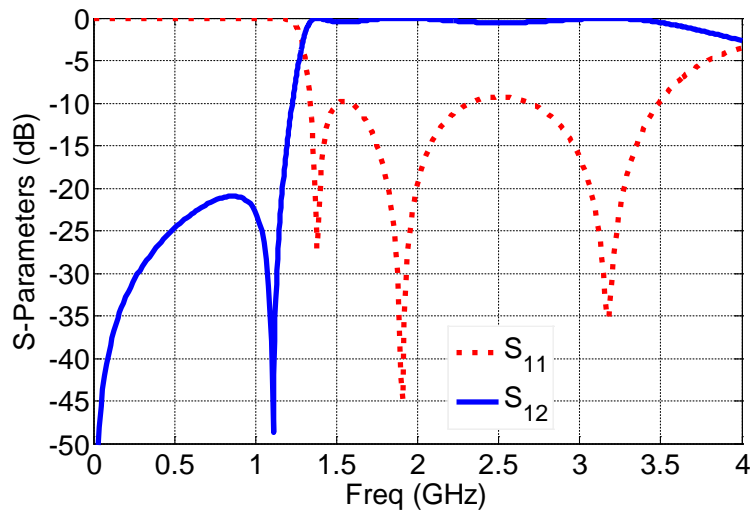


Fig. 8. Simulated frequency responses of the proposed filter.

### III. IMPLEMENTATION AND EXPERIMENTAL RESULTS

A microstrip high-pass filter operating at the frequency range of 1.34 GHz is designed and simulated. The frequency responses of the proposed filter are presented in Fig. 8. To design a high-pass filter based on the proposed procedure, first a MSCSRR with resonance at the central frequency  $f_0=1.34$  GHz is designed. For easy fabrication of the filter, all the gap widths between the interdigital fingers are chosen as 0.2 mm, and the gap widths of the interdigital fingers are also chosen as 0.2 mm.

Table I. Dimensions (in mm) of the proposed high-pass filter.

$l_1=2.2$ mm	$l_2=2$ mm	$l_3=2.2$ mm	$l_4=1.2$ mm
$w=0.2$ mm	$s=0.2$ mm	$g=0.2$ mm	$N=5$ mm
$a=5.4$ mm	$b=5.4$ mm	$c=0.2$ mm	$d=0.2$ mm

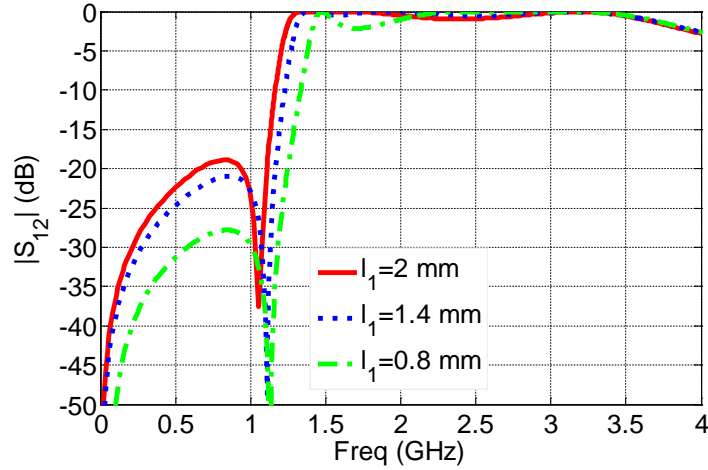


Fig. 9. Simulated frequency responses of the High-Pass filter when length of the interdigital capacitor  $l_1$  are: 0.8, 1.4 and 2 mm respectively.

Dimensions of the proposed high-pass filter which is shown in Fig. 4 are chosen as Table I. The total size of the filter is less than  $0.094 \lambda_g \times 0.045 \lambda_g$  ( $11.2$  mm  $\times$   $5.4$  mm) where  $\lambda_g$  is the guided wavelength at the filter central frequency. The structure has been implemented in the Rogers RO4003C substrate with thickness  $h=0.508$  mm, dielectric constant  $\epsilon=3.55$ . Also in the simulations, the metallic and dielectric loss have been taken into account by using the conductivity of copper  $\sigma=5.8 \times 10^7$  S/m and the loss tangent  $\tan \delta=0.0027$  of the substrate. Thus the proposed high-pass filter has advantages such as small size and low insertion loss. As can be seen in Fig. 9, by reducing the number of the finger in the interdigital capacitor, the high-pass can be easily shifted to higher frequencies and by increasing the number of the finger of the interdigital capacitor, the high-pass can be easily shifted to lower frequencies. Also as be seen in Fig. 10, we can shift the high-pass to higher or lower frequencies by resizing the size of the MSCSRRs.

Consequently, we can easily frequency shift for high-pass by resizing the size of the interdigital capacitor, MSCSRRS and meander lines. The frequency response of the proposed high-pass filter is simulated by using 3-D electromagnetic simulator. Fig. 11 shows the simulated and measured transmission responses of the filter, measured by the employment of a network analyzer Rohde & Schwarz, zvk. The measured cut off frequency is 1.34 GHz. As illustrated in Fig. 12, the group delay is less than 2ns in the cutoff frequency of the proposed high-pass filter.

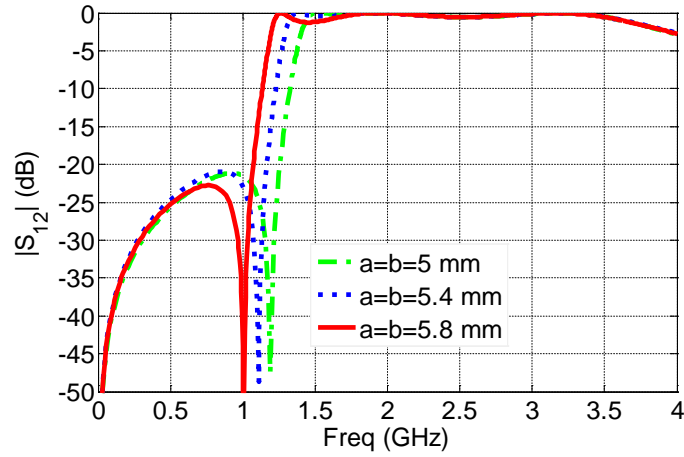


Fig. 10. Simulated frequency responses of the High-Pass filter when the size of the MSCSRR are: 5, 5.4 and 5.8 mm, respectively.

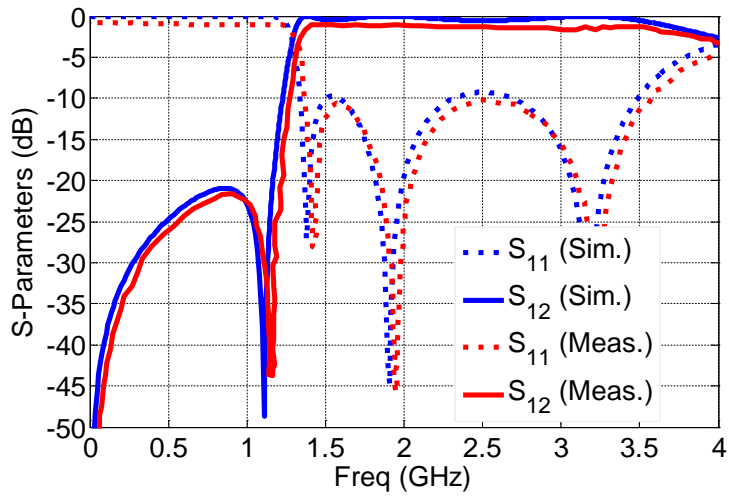


Fig. 11. Simulated and measured frequency responses of the proposed High-Pass filter.

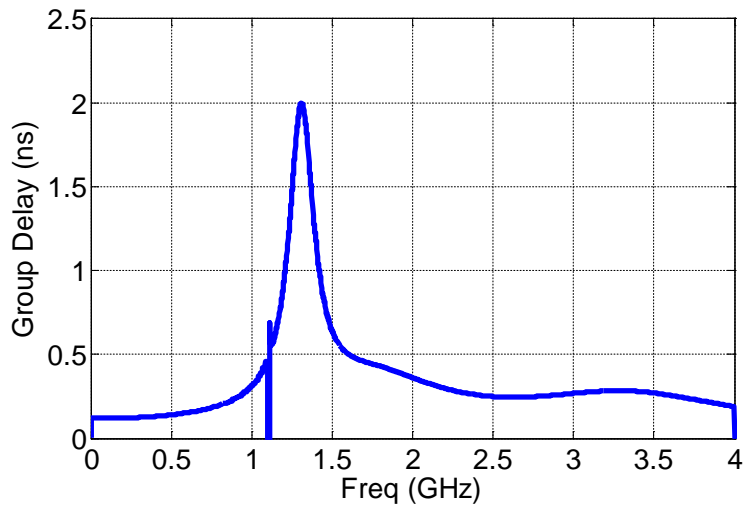


Fig. 12. Simulated group delay of the proposed filter.

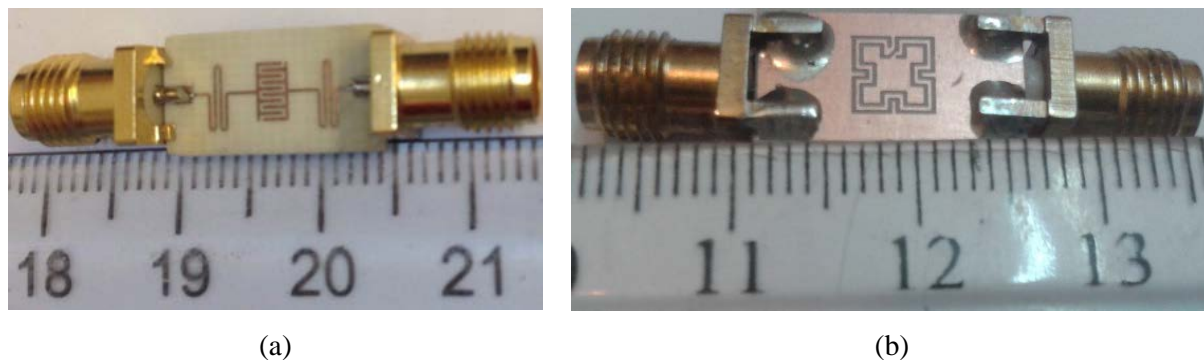


Fig. 13. Top and bottom views of the fabricated high-pass filter.

Table II. Performance comparison of the present filter with the others.

<i>Reference number</i>	<i>f<sub>c</sub> (GHz)</i>	<i>IL(dB)</i>	<i>Rejection in the stopband (dB)</i>	<i>Size (λ<sub>g</sub>×λ<sub>g</sub>)</i>
[12]	5.9	0.81	40	0.086×0.130
[13]	3.0	0.9	20	0.092×0.185
[14]	1.45	2	35	0.325×0.550
[16]	5.7	2	20	1.376×0.294
[17]	16	1.1	38	4.911×2.829
[18]	16	1.5	40	2.805×2.376
<b><i>This Work</i></b>	1.34	1.4	23	0.094×0.045

The photograph of the fabricated filter is shown in Fig. 13 which demonstrates that the designed filter has very small size compared with similar filters. There is good agreement between measurement and simulation results, although there is some deviation, which can be attributed to fabrication related tolerances. The measured return losses are better than 10 dB, and the measured insertion losses are smaller than 1.4 dB. Some minor differences between simulation and measurement results is due to the extra loss from the SMA connectors, by the limited accuracy of fabrication and process of measurement.

Finally, Table II summarizes the comparison of the proposed high-pass filter with other reported microstrip HPFs. In this paper, a HPF in low frequency has been designed because of illustrating the small size of the proposed filter in the lower frequency. Accordingly, the proposed structure have advantages such as compact size, low insertion loss, high return loss, easy bandpass frequency shifting and high Q-factor.

## IV. CONCLUSION

A design procedure for the implementation of a high-pass filter based on the balanced metamaterial TL concept has been proposed. Making use of balanced CRLH based metamaterial transmission lines by etching MSCSRR in the ground plane, high-pass filter is designed. Good performance and small dimensions are achieved. An interdigital capacitor and two meander lines have been considered to implement the series resonant tank, whereas a rectangular MSCSRR has been used for the realization of the parallel resonator. Because of the longer meander slots associated with the MSCSRR particle, the inductance of the proposed unit cell has been increased. Therefore, the electrical size of the proposed structure is decreased and miniaturization is occurred. By choosing suitable values for the parasitic capacitances, a compact and sharp rejection response high-pass filter has been achieved. The designed high-pass filter have been fabricated and measured. The measured results are in a good agreement with the simulation results.

## REFERENCES

- [1] C. Caloz and T. Itoh, *Electromagnetic metamaterials: transmission line theory and microwave applications*, Wiley, New Jersey, 2006.
- [2] R. Marque's, F. Martin and M. Sorolla, *Metamaterials with Negative Parameters*, First Edition, John Wiley Co., 2006.
- [3] F. Martin, *Artificial transmission lines for RF and microwave applications*. John Wiley & Sons, 2015.
- [4] I. Bahl, *Lumped elements for RF and microwave circuits*, Artech House, Inc., 2003.
- [5] M. Gil, J. Bonache, J. Selga, J. Garcia-Garcia, and F. Martin, "Broadband resonant-type metamaterial transmission lines." *IEEE Microwave and Wireless Components Letters*, vol. 17, no. 2, pp. 97-99, 2007.
- [6] M. Anoniades and G.V. Eleftheriades, "Compact linear lead/lag metamaterial phase shifters for broadband applications," *IEEE Antennas Wireless Propagation Lett*, vol. 2, no. 5, pp.103-106, 2003.
- [7] C. Caloz, A. Sanada, and T. Itoh, "A novel composite right-/left handed coupled-line directional coupler with arbitrary coupling level and broad bandwidth," *IEEE Trans Microwave Theory Tech*, vol. 52, no.1, pp. 980-992, 2004.
- [8] M. Duran-Sindreu, A. Velez, F. Aznar, G. Siso, J. Bonache, and F. Martin, "Applications of open split ring resonators and open complementary split ring resonators to the synthesis of artificial transmission lines and microwave passive components," *IEEE Trans Microwave Theory Tech*, vol. 57, no.4, pp. 3395-3403, 2009.
- [9] M. Gil, J. Bonache, J. Martel, and F. Martin, "Composite right/left handed metamaterial transmission lines based on complementary split-rings resonators and their applications to very wideband and compact filter design," *IEEE Trans Microwave Theory Tech*, vol. 55, no.2, pp. 1296-1304, 2007.
- [10] W. Tong, H. Zhang, and Z. Hu, "A 3D multilayered Si MMIC left handed metamaterial bandpass filter, in IEEE International Symposium on Radio-Frequency Integration Technology," *RFIT*, vol. 55, no. 6, pp. 137-139, 2009.
- [11] M. Duran-Sindreu, P. Velez, J. Bonache, and F. Martin, "Broadband microwave filters based on metamaterial concepts," In *2010 Conference Proceedings, ICE Com*, 20-23 September 2010.
- [12] Chen, Hui, Ke-Song Chen, Di Jiang, and Hong-Fei Zhao, "A Compact Dual-Metal-Plane High-pass Filter Using Hybrid Microstrip/DGS," *Progress in Electromagnetics Research Letters*, vol. 60, no. 3, pp. 53-58, 2016.
- [13] M. Duran-Sindreu, J. Bonache, and F. Martin, "Elliptic high-pass filters with stepped impedance resonators in coplanar waveguide technology," *Microwave and Optical Technology Letters*, vol. 54, no. 4, pp. 1094-1097, 2012.

- [14] J. Selga, M. Gil, F. Aznar, J. Bonache, and F. Martin, "Composite right-/left-handed coplanar waveguides loaded with split ring resonators and their application to high-pass filters," *IET microwaves, antennas & propagation*, vol. 4, no. 7, pp. 822-827, 2010.
- [15] D. M. Pozar, *Microwave Engineering*, 4<sup>th</sup> Edition, John Wiley, 2012.
- [16] M. A. Rabah, M. Abri, H. Abri Badaoui, J. Tao, and T.-H. Vuong, "Compact miniaturized half-mode waveguide/high pass-filter design based on SIW technology screens transmit-IEEE C-band signals," *Microwave and Optical Technology Letter*, vol. 58, no. 2, pp. 414-418, 2016.
- [17] X. Juan, Z. Li, and R. Chen, "Optimization of a novel substrate integrated waveguide high-pass filter using space mapping," *Microwave and Optical Technology Letters*, vol. 57, no. 3, pp. 733-737, 2015.
- [18] X. Juan, J. Bi, Z. Li, and R. Chen, "Substrate integrated waveguide high-pass filter with high selectivity," *Electronics Letters*, vol. 51, no. 14, pp. 1080-1082, 2015.